# Multimodality Imaging of Neuroendocrine Tumors

Samuel J. Galgano, MD[a,b,*], Kedar Sharbidre, MD[a], Desiree E. Morgan, MD[a]

**KEYWORDS**

• Neuroendocrine tumor • DOTATATE • PET • CT • MR imaging • Carcinoid

**KEY POINTS**

- Neuroendocrine tumors are a heterogeneous group of tumors and knowledge of pathology is essential to selecting the appropriate imaging modality.
- DOTATATE-PET/computed tomography scans offer substantial improvement for systemic staging of well-differentiated neuroendocrine tumors compared with computed tomography scans and MR imaging and offer potential value for theranostic applications.
- Neuroendocrine tumors can occur as part of systemic syndromes, such as multiple endocrine neoplasia, and detection of 1 neoplasm may prompt additional screening for other neuroendocrine neoplasms.

## INTRODUCTION

Neuroendocrine tumors (NET) are a rare type of solid tumor with an estimated 12,000 people in the United States diagnosed with a NET each year and approximately 170,000 people living with a NET.[1] In the past several decades, the incidence rate of NETs has continued to increase, with a 6.4-fold increase between 1973 and 2012.[1] This increase is thought to be in part owing to an increased awareness of NETs, but largely attributed to improvements medical imaging and endoscopy (including endoscopic ultrasound). There is a wide spectrum of disease in NETs, ranging from slow-growing and indolent tumors that are incidentally found on imaging for unrelated clinical indications to highly aggressive malignancies with a poor prognosis. Despite the increase in the prevalence and detection of NETs, significant improvements in overall survival have been observed since 2000. In 2018, the US Food and Drug Administration approved a targeted systemic therapy to somatostatin receptor (SSTR)-expressing gastroenteropancreatic NETs (GEP-NETs).[1] The focus of this article is on the evaluation, detection, and staging of the most common types of NETs with multiple imaging modalities, because the information gained with a multimodality approach is often complementary and leads to image-guided treatment decision making at a patient-specific level. Additionally, given the spectrum of pathology in NETs, the article briefly addresses key pathologic issues that guide imaging evaluation in patients with NETs.

## IMAGING PROTOCOLS

### *Computed Tomography Scans and MR Imaging*

The current American College of Radiology Appropriateness Criteria for neuroendocrine imaging focuses only on pituitary imaging, which are covered in a different chapter of this book.[2] However, no American College of Radiology Appropriateness Criteria exist to describe appropriate imaging of NETs in the chest, abdomen, and pelvis.

[a] Department of Radiology, Section of Abdominal Imaging, University of Alabama at Birmingham, 619 19th Street South, JT N325, Birmingham, AL 35249, USA; [b] Department of Radiology, Section of Molecular Imaging & Therapeutics, University of Alabama at Birmingham, 619 19th Street South, JT N325, Birmingham, AL 35249, USA

* Corresponding author. Department of Radiology, Section of Abdominal Imaging, University of Alabama at Birmingham, 619 19th Street South, JT N325, Birmingham, AL 35249.
*E-mail address:* samuelgalgano@uabmc.edu

Radiol Clin N Am 58 (2020) 1147–1159
https://doi.org/10.1016/j.rcl.2020.07.008

Multidetector computed tomography (CT) scanning is widely used in the assessment of pancreatic NETs with detection rates of up to 69% to 94%.[3] On dual phase pancreatic CT protocols used to evaluated suspected pancreatic masses, NETs are typically hypervascular and demonstrate avid enhancement in the arterial phase. This factor is especially important in the diagnosis of liver metastases from NET. Some studies have shown that the contrast enhancement pattern of NETs can correlate with the tumor grade. Cappelli and colleagues[4] showed that tumors with venous and delayed phase enhancement are likely to be high grade compared with tumors with arterial enhancement and venous phase washout. Other findings, such as tumor size, ill-defined tumor margins, pancreatic duct dilation, and vascular invasion, have also been found to be significant in predicting grading of tumors. Dual energy CT scans can help to improve the detection of small pancreatic NETs, particularly using low-energy monochromatic and iodine density images.[5] For assessment of small bowel NETs, CT scans and MR enterography protocols are used with unenhanced images, followed by arterial and venous phase acquisitions after distension of the bowel by neutral contrast. Recent studies have shown that CT scans and MR enterography have higher sensitivity (100% and 86%–94%, respectively) and specificity (96.2% and 95%–98%, respectively) for the detection of small bowel neoplasms, including NETs.[6,7]

Owing to its superior soft tissue characterization, MR imaging has an improved detection rate compared with CT, particularly for the characterization of previously indeterminate pancreatic lesions.[8] Additional sequences such as diffusion-weighted imaging and apparent diffusion coefficient mapping can help to localize and potentially grade the tumors.[9–11] MR cholangiopancreatography is useful to evaluate the status of pancreatic duct and biliary system and should be performed for surgical planning.[12] Other focal pancreatic lesions like hypervascular metastasis, intrapancreatic accessory splenule, or serous cystadenoma can be sometimes be confused with NETs, and MR imaging can aid with problem solving in such cases.[13,14]

## [$^{68}$Ga]DOTATATE PET/Computed Tomography Scans and PET/MR Imaging

[$^{68}$Ga]DOTATATE was approved in 2016 for the localization of SSTR-positive NETs in adult and pediatric patients.[15] Once injected, DOTATATE binds to SSTRs on the cell surface, with highest affinity for the SSTR2 receptor.[16] Clinically, [$^{68}$Ga]DOTATATE-PET/CT is rapidly becoming the standard of care in the evaluation of NET, owing to its superior sensitivity and specificity for detection of metastatic disease when compared with [$^{111}$In]pentetreotide scintigraphy.[17] Frequently, the findings from a [$^{68}$Ga]DOTATATE-PET/CT are complementary to CT and MR imaging, which offer higher spatial resolution and aid in surgical planning and decision-making. As peptide receptor radionuclide therapy (PRRT) with [$^{177}$Lu]DOTATATE becomes increasingly available and offered to patients, [$^{68}$Ga]DOTATATE-PET/CT is essential to assess patient eligibility before PRRT. Finally, as the emerging hybrid imaging modality PET/MR imaging becomes increasingly available, [$^{68}$Ga]DOTATATE-PET/MR imaging allows for synchronous acquisition of both PET and MR imaging data with excellent anatomic co-registration and may allow for simultaneous assessment of metastatic disease using both [$^{68}$Ga]DOTATATE-PET and diagnostic contrast-enhanced MR imaging of the abdomen (**Fig. 1**).

[$^{68}$Ga]DOTATATE-PET scans require preparation of the radiopharmaceutical before injection into the patient. The radionuclide [$^{68}$Ga] is eluted from a [$^{68}$Ge] generator and has a half-life of 68 minutes, which somewhat limits its ability to be commercially distributed compared with [$^{18}$F], which has a half-life of 110 minutes. The recommended dose of [$^{68}$Ga]DOTATATE is 2 MBq/kg (0.054 mCi/kg) up to 200 MBq (5.4 mCi). Patients are instructed to be well-hydrated before performance of the PET scan and are advised to void frequently after injection of radiotracer to decrease radiation exposure. Approximately 40 to 90 minutes following injection of [$^{68}$Ga]DOTATATE, patients can be scanned with a typical field-of-view from skull base to the mid thigh.

## [$^{111}$In]Pentetreotide Scintigraphy

Before the approval of [$^{68}$Ga]DOTATATE for imaging of NETs, [$^{111}$In]pentetreotide (Octreoscan; Covidien Inc., Dublin, Ireland) was the standard of care for molecular imaging of NETs.[18] The mechanism of action of pentetreotide is the binding of SSTRs at the cell surface, albeit with a lower affinity than [$^{68}$Ga]DOTATATE. Additionally, owing to the gamma emission of 171 keV and 245 keV photons from [$^{111}$In] during its decay, imaging is limited to planar and single photon emission CT (SPECT) or SPECT/CT images on a gamma camera. The half-life of [$^{111}$In] is 2.8 days, and images obtained during [$^{111}$In]pentetreotide scintigraphy are routinely acquired at 24 hours after injection, with optional imaging at 4 and 48 hours after injection. This nature leads to patients having to return

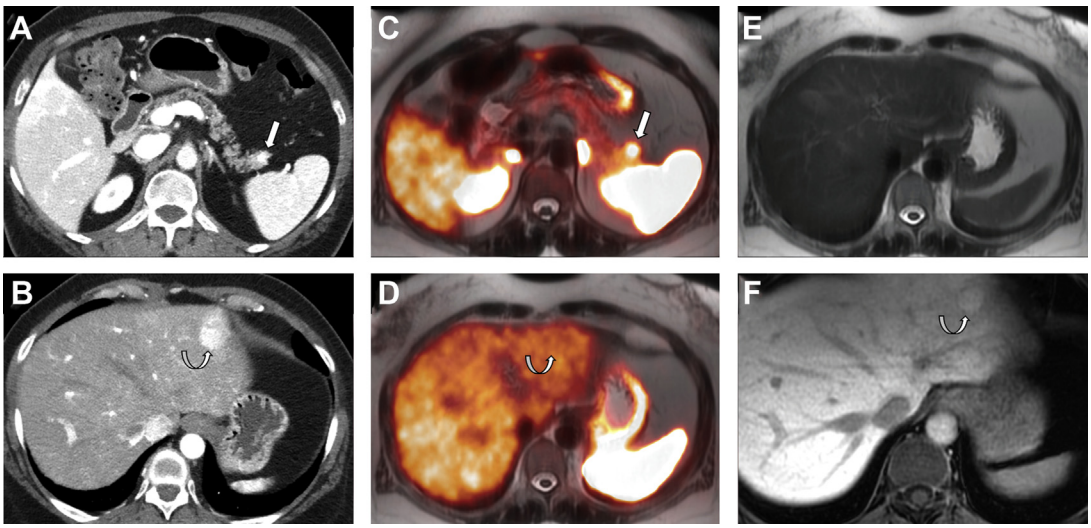


**Fig. 1.** Patient with suspected pancreatic tail NET on contrast-enhanced portal venous phase CT scan (*A*) and possible hepatic metastasis on contrast-enhanced arterial-phase CT scan (*B*). Subsequent [$^{68}$Ga]DOTATATE-PET/MR imaging shows focal activity (*arrow*) in the pancreatic tail NET (*C*) and no activity in the suspected liver metastasis (*curved arrow*) (*D*). Corresponding T2-weighted (*E*) and hepatobiliary phase T1-weighted postcontrast MR images (*F*) demonstrate no increased T2 signal in the liver lesion, which demonstrates hepatobiliary phase contrast retention (*curved arrow*), consistent with focal nodular hyperplasia.

to the nuclear medicine department multiple times, which is a significant drawback when compared with [$^{68}$Ga]DOTATATE-PET/CT. Although an important historical radiotracer that provided key diagnostic information about NETs, current use of [$^{111}$In]pentetreotide is limited to practice settings with limited or no access to [$^{68}$Ga]DOTATATE and has been shown to be an inferior molecular imaging agent.[17]

## PATHOLOGY AND IMAGING CONSIDERATIONS

### *Variable Somatostatin Receptor Expression Among Neuroendocrine Tumors*

It is well-known that NETs are a heterogeneous group of tumors and that certain NETs overexpress different SSTR subtypes at the cell surface.[19–21] Historically, [$^{111}$In]pentetreotide scintigraphy preferentially localized to the SSTR2 and SSTR5 receptors, which are upregulated in pheochromocytomas, gastrinomas, glucagonomas, and nonfunctional GEP-NETs. However, both insulinomas and medullary thyroid cancer demonstrate variable levels of SSTR expression, particularly the SSTR2 receptor.[22,23] As a result, studies of [$^{111}$In]pentetreotide scintigraphy demonstrated low sensitivity for the detection of medullary thyroid cancer and insulinomas.[24–26] [$^{68}$Ga]DOTATATE-PET/CT scanning has demonstrated significant improvement in detection of insulinomas owing to the higher cell receptor binding and spatial resolution of the PET radiotracer.[27] Thus, when performing a molecular imaging study to evaluate for either primary or metastatic NET, it is essential that the interpreting physician know the suspected pathology of the tumor and the potential limitations of the examination, particularly if performing [$^{111}$In]pentetreotide scintigraphy. Additionally, certain NETs (such as gastrinoma) occur in characteristic anatomic locations (eg, the gastrinoma triangle), and providing this information to the interpreting physician can allow for greater scrutiny of the scan in the areas of concern.

### *Neuroendocrine Tumor Differentiation and Choice of Molecular Imaging Agent*

Another key pathologic consideration in molecular imaging of NETs is the degree of pathologic differentiation, because it may influence the choice of molecular imaging agent. NETs are classified by the 2017 World Health Organization into 3 pathologic grades (G1–G3) on the basis of the number of mitoses seen on high-powered microscopy, the Ki-67 index, and the presence or absence of tumor necrosis and apoptosis.[28] As an example, G1 NETs are well-differentiated with extremely low Ki-67 (<3%), low number of mitoses, and rare tumor necrosis. The 2017 World Health Organization criteria also introduced a separate subtype of poorly differentiated neuroendocrine carcinoma, which also has large cell and small

cell variants, and renamed mixed neuroendocrine or non-neuroendocrine neoplasms.[29] In regard to the selection of PET radiotracers, knowledge of the pathology is paramount, because more aggressive tumors may be better imaged with PET scanning with [$^{18}$F]fluorodeoxyglucose (FDG-PET)/CT scanning rather than [$^{68}$Ga]DOTATATE-PET/CT, owing to their more aggressive cellular behavior and poor differentiation, which together result in decreased expression of SSTRs at the cell surface. In cases of G2 NETs, both [$^{18}$F]FDG-PET/CT scans and [$^{68}$Ga]DOTATATE-PET/CT scans may be performed before therapeutic intervention, as differential uptake on these 2 examinations may influence therapeutic management between PRRT, systemic chemotherapy, and/or surgery. Thus, interpreting physicians should take caution when interpreting [$^{68}$Ga]DOTATATE-PET/CT without pathologic data, because low expression in a known NET or suspected metastasis could represent a poorly differentiated NET and may require a [$^{18}$F]FDG-PET/CT for adequate staging (**Fig. 2**).

## GASTROENTEROPANCREATIC NEUROENDOCRINE TUMORS

The gastrointestinal tract and pancreas are the most common locations (about 70%) for NETs.[30] GEP-NETs account for about 1.5% to 2.0% of all primary gastrointestinal and pancreatic neoplasms, and their incidence in the United States is estimated at 3.56 per 100,000 population.[1] The majority of these cases are sporadic, and a small percentage occur in patients with genetic syndromes such as multiple endocrine neoplasia type 1 (MEN-1), neurofibromatosis type 1, Von Hippel-Lindau disease, and tuberous sclerosis complex.

Pancreatic NETs account for about 1% to 2% of all pancreatic neoplasms with an incidence of less than 1%, al though increasing over the last 20 to 30 years.[31] Functioning pancreatic NETs are diagnosed earlier because of the symptoms, but are less common (10%–30%) than nonfunctioning tumors. Among functional NETs, insulinomas are the most common tumors, followed by gastrinomas.[32] The nonfunctioning tumors produce nonspecific symptoms. Because of slow growth and late detection, these tumors can have an advanced stage when diagnosed.[33,34] In patients with functioning NETs, laboratory analyses of the specific hormone levels are often diagnostic and can be tested in urine or serum. Chromogranin A is the most commonly used serum marker for diagnosis and is found to be elevated in 60% to 80% patients.[13,35]

The gastrointestinal tract is the most common site of NETs (67%); the distal part of the ileum being the most common location.[36] The majority of ileal NETs are hormonally inactive and can present as vague abdominal pain, gastrointestinal bleeding, or bowel obstruction. Classic carcinoid syndrome (diarrhea, tachycardia, hot flushes, and skin reddening) is seen in 6% to 30% of patients and more commonly occurs (about 95% of cases) with hepatic metastasis.[35] Gastric NETs are rare and account for approximately 0.3% of gastric tumors. Three distinct types of gastric NETs have been described, of which type I and II are asymptomatic and generally manifest as multiple small polyps in gastric fundus and body, incidentally diagnosed on endoscopy[37] (**Fig. 3**). Type III gastric NETs demonstrate marked enhancement and can have an infiltrative appearance on imaging. Duodenal NETs are most commonly gastrinomas, and one-third of these tumors develop Zollinger-Ellison syndrome owing to excess gastrin

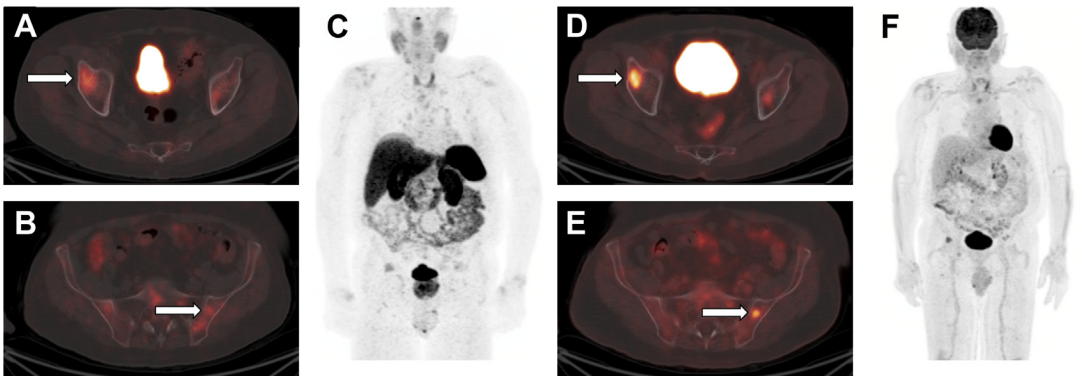


**Fig. 2.** Patient with metastatic NET demonstrating low activity (*arrow*) on fused [$^{68}$Ga]DOTATATE-PET/CT images (*A*, *B*) and maximum intensity projection image (*C*). Subsequent [$^{18}$F]FDG-PET/CT images (*D–F*) demonstrate substantially higher FDG activity (*arrow*) than [$^{68}$Ga]DOTATATE-PET/CT, indicating poorly differentiated histology.

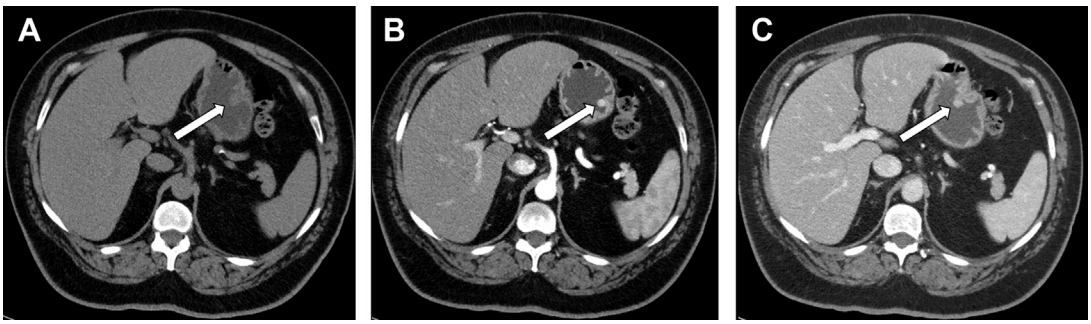


Fig. 3. CT images in noncontrast (*A*), arterial (*B*), and portal venous (*C*) phases demonstrate a small enhancing polyp in the stomach (*arrow*), subsequently biopsied and found to represent gastric NET.

secretion. Multiple gastrinomas are more commonly seen in patients with MEN-1 syndrome.

Functioning NETs are usually smaller in size (1–2 cm), well-defined, and hypervascular (Fig. 4). Insulinomas are typically solitary and smaller compared with other functioning NETs. Gastrinomas are located in the gastrinoma triangle, which is bounded by the cystic duct junction with the common bile duct, the pancreatic neck, and the junction of the second and third portions of the duodenum; 60% tumors found in pancreas, and remainder are seen in duodenum or peripancreatic lymph nodes. Those within the duodenum are usually multiple, subcentimeter in size, and better detected by endoscopic ultrasound imaging rather than CT scans or MR imaging.

Nonfunctioning NETs are usually larger in size, may be symptomatic owing to the mass effect, have encapsulated margins, and show heterogeneous enhancement, often characterized by areas of cystic degeneration, necrosis, or sometimes fibrosis (Fig. 5). Cystic degenerated NETs are seen in up to 17% of cases, and more commonly in patients with MEN-1 syndrome. The presence of a hypervascular rim on CT scanning or MR imaging can help to suggest the diagnosis compared with other cystic pancreatic masses.[38] Both functioning and nonfunctioning NETs very rarely involve the main pancreatic duct to cause duct dilation, a finding commonly seen in patients with pancreatic adenocarcinoma. Pancreatic NETs usually metastasize to liver and regional lymph nodes, whereas locally invasive tumors can extend into the retroperitoneum.

On CT scans and MR imaging, small bowel NETs may present as polypoid hypervascular masses or focal concentric bowel wall thickening. More often, NETs are diagnosed by detection of a mesenteric mass with a surrounding desmoplastic reaction owing to local effects of serotonin. Smaller NETs of the small bowel are difficult to diagnose and may present with only metastatic disease. Appendiceal NETs are incidentally discovered during appendicectomy in 70% cases, have a favorable prognosis compared with other NETs, and metastasize less frequently. As with other GEP-NETs, appendiceal NETs are seen as small arterial hyperenhancing lesions on CT scans and MR imaging and are typically located in the appendiceal tip. Uncommonly, NETs may arise in the colon and rectum, accounting for about 11% of all GEP-NETs.[36] The majority of these tumors are incidentally detected on colonoscopy, but occasionally patients may present with gastrointestinal bleeding and pain.

Nodal staging of NETs is usually performed by CT scan, MR imaging, or PET imaging. Like the primary lesions, nodal metastases are also typically


Fig. 4. CT images in arterial (*A*) and portal venous (*B*) phases demonstrate a small well-circumscribed avidly enhancing mass in the pancreatic tail (*arrow*), likely a NET. Fused image from subsequent [$^{68}$Ga]DOTATATE-PET/CT (*C*) demonstrates avid tracer activity in the lesion, consistent with pancreatic NETs.

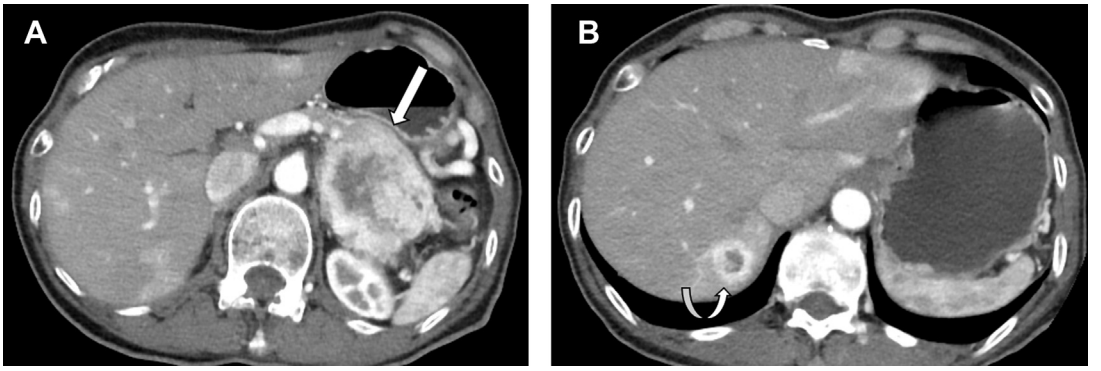


**Fig. 5.** CT images in the arterial phase demonstrate a large heterogeneous enhancing mass (*arrow*) arising from the pancreatic tail (*A*) with a similar appearing metastatic lesion (*curved arrow*) in the liver (*B*). Subsequent biopsy confirmed nonfunctional metastatic pancreatic NETs.

hypervascular and more conspicuous on arterial phase. Liver metastases are also typically hypervascular in arterial phase; lesions with hypoenhancement in all phases suggest a poor prognosis.[39] MR imaging is a more sensitive modality compared with CT scans for the detection of NET liver metastases. Dynamic contrast-enhanced MR imaging, in particular using gadoxetic acid and diffusion-weighted imaging, is helpful in increasing diagnostic confidence for liver metastasis detection.

Somatostatin receptor imaging has long been a part of the diagnosis and staging for GEP-NETs. The initial experience with [$^{111}$In]pentetreotide demonstrated a similar sensitivity, specificity, and accuracy between helical CT scans and somatostatin receptor scintigraphy.[40] The performance of [$^{111}$In]pentetreotide somatostatin receptor scintigraphy is increased when performed as an SPECT/CT scans compared with SPECT scans or planar scintigraphy alone.[41] However, given advances in CT scans and MR imaging technology and acquisition techniques, CT scanning and MR imaging now perform better than [$^{111}$In]pentetreotide, and the use of somatostatin receptor scintigraphy should be limited to cases in which disease is occult on CT or MR imaging.[42] More recently, US Food and Drug Administration approval of [$^{68}$Ga]DOTATATE and [$^{177}$Lu]DOTATATE has substantially altered the imaging diagnosis, management, and treatment of GEP-NETs. Multiple studies have shown superior performance of [$^{68}$Ga]DOTATATE-PET/CT scans compared with [$^{111}$In]pentetreotide somatostatin receptor scintigraphy, resulting in changes in treatment plans in up to 36% of patients who underwent both scans.[17,43,44] Given the superior performance of [$^{68}$Ga]DOTATATE-PET/CT scans among molecular imaging agents and the potential for targeted molecular therapy with [$^{177}$Lu]DOTATATE PRRT, this approach is the current favored method of systemic staging for patients with NETs before treatment.

## LUNG AND THYMIC CARCINOID TUMORS

Lung carcinoid tumors account for approximately 1% to 2% of all lung cancers, with approximately 2000 to 4500 newly diagnosed cases in the United States each year.[45] Lung carcinoid tumors are classified as typical or atypical, with typical lung carcinoid tumors arising in slightly younger patients (the average age at diagnosis is 45 years).[45] Lung carcinoid tumors are generally classified as well-differentiated NETs and are often slow growing with a benign clinical courses.[45–47] Frequently, lung carcinoid tumors are endobronchial lesions that present with symptoms of cough, hemoptysis, or pneumonia secondary to bronchial obstruction from the lesion.[46] Thymic carcinoid tumors (also referred to as NETs of the thymus) are rare tumors, accounting for only 2% to 5% of thymic tumors and 0.4% of all carcinoid tumors, with an estimated incidence of 0.2 per million in the United States.[48,49] Thymic NETs are associated with the genetic syndrome MEN-1. Thymic carcinoid tumors have heterogeneous clinical behaviors and pathologic appearances, ranging from asymptomatic and nonaggressive to symptomatic and highly aggressive.[50] If symptomatic, patients often present secondary to symptoms of mass effect or invasion of the mediastinal structures; carcinoid syndrome is an uncommon clinical presentation.[46,51] Interestingly, up to 50% of patients with thymic carcinoid tumors have hormonal abnormalities, the most frequent being Cushing syndrome secondary to primary tumoral secretion of adenocorticotropic hormone.[52] Up to 30% of

patients with thymic carcinoid present with advanced-stage disease, much higher than lung carcinoid tumors.

Given the general benign course of many lung carcinoid tumors, these lesions are frequently incidentally detected on CT scans of the chest performed for other reasons. Approximately 60% to 70% of lung carcinoids arise in the central airways and involve the main, lobar, or segmental bronchi.[46] These centrally located tumors are more frequently typical carcinoid tumors, but the imaging features of both typical and atypical lung carcinoid tumors overlap and are too similar for confident differentiation on CT scan. Chest radiography often shows a well-defined hilar or perihilar mass with or without the presence of distal airspace disease. When carcinoid tumors arise distal to the segmental bronchi in the lung, these are termed peripheral carcinoids and are more frequently atypical on histology.[46] These carcinoid tumors are typically appear as a well-circumscribed slightly lobulated spherical or ovoid nodule or mass with the long axis parallel to adjacent bronchi or pulmonary artery branches. On CT scans, up to 30% of lung carcinoid tumors demonstrate punctate or diffuse calcifications and may demonstrate avid vascularity and internal enhancement. For endobronchial carcinoid tumors, evaluation with thin section CT chest scanning is useful to establish the relationship between the lesion and the bronchi, and can aid in directing bronchoscopic evaluation and biopsy (**Fig. 6**). Mediastinal and hilar adenopathy is a common finding on CT scans and may be reactive secondary to recurrent pneumonia versus lymph node metastases, the latter being more common with atypical carcinoids.[53,54] Thymic carcinoids arise in the anterior mediastinum and on CT scanning may mimic a thymoma.[55] The appearance of thymic carcinoid is overall nonspecific, but these masses tend to be large, ranging from 6 to 20 cm, and demonstrate heterogeneous enhancement and locally aggressive features.[56] Scattered calcifications may be present within thymic carcinoids.[57] MR imaging is seldom used for the evaluation of pulmonary nodules and masses, but may be used in the evaluation of mediastinal or thymic lesions to assist in the characterization of the internal components. Small case series report that primary thymic NETs are isointense to mildly hyperintense to skeletal muscle on T1-weighted images and heterogeneously T2 hyperintense.[57]

Historically, carcinoid tumors of the lung have been evaluated with several types of radiotracers, including [$^{111}$In]pentetreotide, [$^{18}$F]FDG, and most recently [$^{68}$Ga]DOTATATE. A study comparing the performance of [$^{111}$In]pentetreotide SPECT/CT scans with contrast-enhanced CT scans demonstrated increased sensitivity (96.0% vs 87.5%, respectively) with slightly less specificity (92% vs 97%, respectively) for detection of the primary lesion or recurrent disease.[58] As with other radiotracers imaged with SPECT/CT scans, a known limitation of the imaging modality is decreased spatial resolution when compared with a standard diagnostic contrast-enhanced CT scan. [$^{111}$In]Pentetreotide has been studied in evaluation of thymic tumors, many of which demonstrate increased SSTR expression. Although [$^{111}$In]pentetreotide is able to accurately exclude a diagnosis of thymic hyperplasia, it is unable to differentiate between other thymic tumors owing to overexpression of SSTRs.[59] An [$^{18}$F]FDG-PET/CT scan is a frequently performed examination during the initial evaluation of solid pulmonary nodules and for staging of known lung cancer. Given the difficulty differentiating lung carcinoid tumors from other etiologies of pulmonary nodules, there are frequently initially evaluated with [$^{18}$F]FDG-PET/CT. Although typical lung carcinoid tumors have less FDG uptake than other lung malignancies, atypical lung carcinoid tumors frequently demonstrate marked FDG uptake and seem to be similar to other primary lung malignancies[60–62] (**Fig. 7**). Neuroendocrine neoplasms, including lung carcinoids, which demonstrate high metabolic tumor volume on [$^{18}$F]FDG-PET/CT scans are associated with poor survival given their more aggressive histologic features.[63] [$^{68}$Ga]DOTATATE-PET/CT scans (and other DOTA-peptide PET/CT imaging) has shown promising results for lung carcinoid tumors, particularly

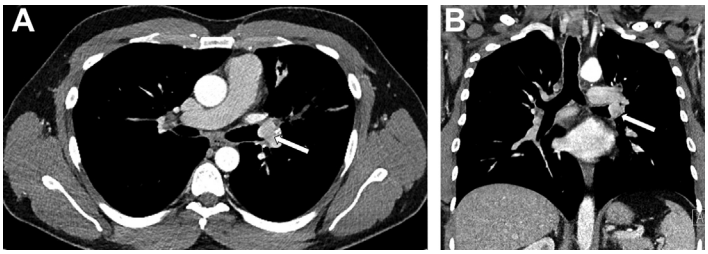


**Fig. 6.** Axial (*A*) and coronal (*B*) contrast-enhanced CT images of the chest demonstrate an avidly enhancing endobronchial lesion in the left mainstem bronchus (*arrow*), consistent with a lung carcinoid.

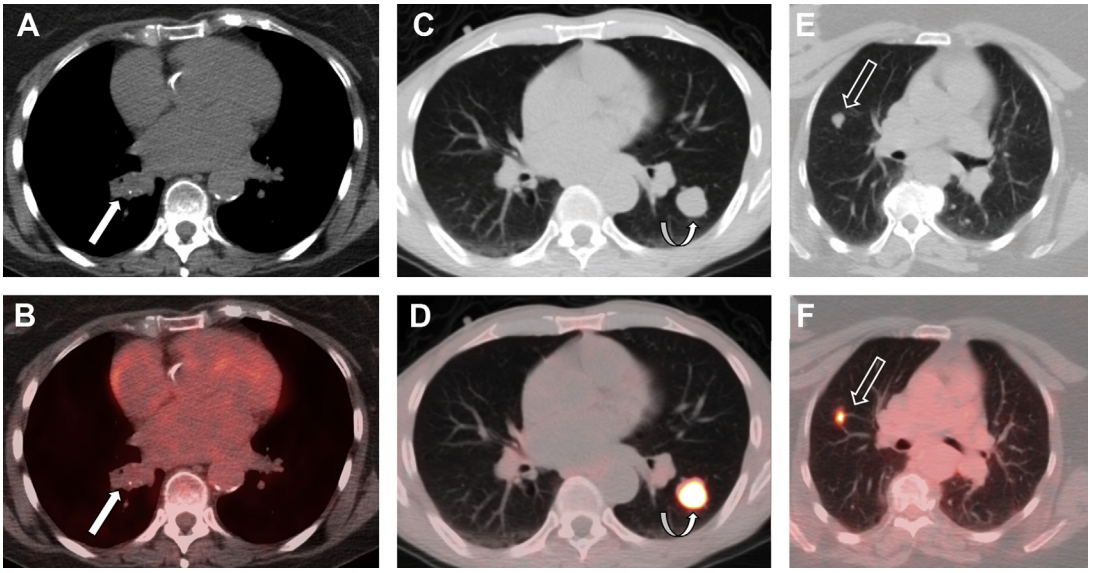


Fig. 7. Three patients with lung carcinoid tumors. Axial CT (*A*) and fused [$^{18}$F]FDG-PET/CT (*B*) images demonstrate a right-sided endobronchial lesion (*arrow*) with calcifications and low FDG uptake, biopsy-proven to represent a typical lung carcinoid. Axial CT (*C*) and fused [$^{68}$Ga]DOTATATE-PET/CT (*D*) images from a different patient demonstrate a well-circumscribed left nodule (*curved arrow*) with very high tracer activity, consistent with a typical lung carcinoid. Axial CT (*E*) and fused [$^{18}$F]FDG-PET/CT (*F*) images from a third patient demonstrate increased tracer activity in a peripheral right lung nodule (*open arrow*), which was subsequently biopsied and found to represent an atypical lung carcinoid.

typical carcinoids[17] (see Fig. 7). [$^{68}$Ga]DOTATATE-PET/CT scanning has been shown to have superior diagnostic performance when compared with [$^{18}$F]FDG-PET/CT scans in the evaluation of typical pulmonary carcinoid, while an [$^{18}$F]FDG-PET/CT scan is superior in the evaluation of atypical pulmonary carcinoid.[60,64] Thus, in the initial molecular imaging evaluation of patients with lung carcinoid tumors of unknown histology, both [$^{18}$F]FDG and [$^{68}$Ga]DOTATATE imaging can be performed for a comprehensive initial evaluation; knowledge of pathologic findings is key to determining which radiotracer is more suitable for both initial staging and follow-up PET/CT examinations.

## PHEOCHROMOCYTOMA AND PARAGANGLIOMA

Paragangliomas and pheochromocytomas are rare neuroendocrine neoplasms with a combined estimated annual incidence of approximately 0.8 per 100,000 person-years; between 500 and 1600 cases are diagnosed in the United States each year.[65,66] However, given the nonfunctional behavior of many paragangliomas, autopsy series suggest that the prevalence may be higher than reported owing to undiagnosed tumors.[67] Many paragangliomas are diagnosed in the third to fifth decades with a mean age of diagnosis of 47 years.[68] Paragangliomas are associated with the genetic syndromes MEN 2A and 2B, neurofibromatosis type, hereditary paraganglioma-pheochromocytoma syndrome, and von Hippel Lindau disease (Fig. 8). In these patients with a genetic predisposition to develop paragangliomas and pheochromocytomas, the mean age of diagnosis is younger than those diagnosed with sporadic paragangliomas. These tumors may arise from either the sympathetic or parasympathetic paraganglia in the head, neck, skull base, adrenal gland, or along the abdominopelvic sympathetic chain. These lesions may be nonsecretory or secrete catecholamines (commonly referred to as pheochromocytomas), and they are classified by the World Health Organization (2004) by anatomic site of origin, regardless of secretory status. When secretory, catecholamine-secreting paragangliomas present with severe hypertension and other symptoms related to excess catecholamine. However, the vast majority of paragangliomas are nonsecretory and are either incidentally discovered or produce symptoms secondary to local mass effect, particularly in the head, neck, and skull base. Approximately 26% of paragangliomas are multiple (more common in hereditary cases), 15% to 20% are extra-adrenal, and 33% to 50% are associated with a hereditary syndrome.[69] Rates of malignant paragangliomas vary by

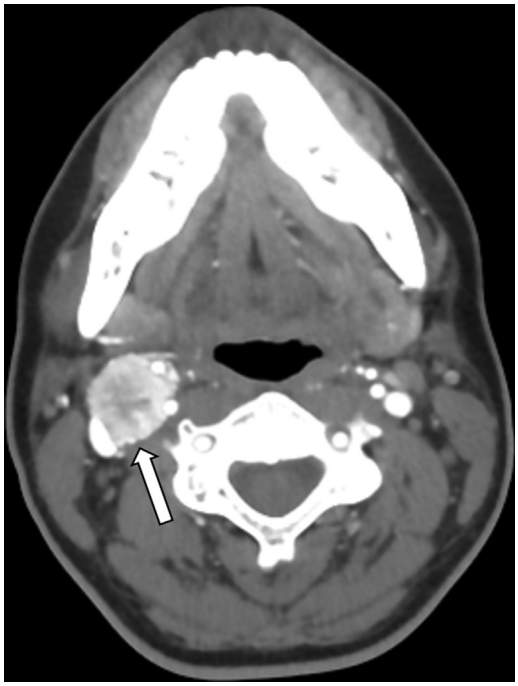

**Fig. 8.** Axial contrast-enhanced CT image demonstrating an avidly enhancing mass (*arrow*) in the right carotid space with splaying of the internal and external carotid arteries, characteristic of a carotid body paraganglioma. The patient subsequently underwent genetic testing and was found to have hereditary paraganglioma–pheochromocytoma syndrome secondary to a *SDHB* mutation.

anatomic location, with approximately 20% of extra-adrenal secretory paragangliomas being malignant and most skull base and neck paragangliomas being benign.[70,71]

The initial imaging evaluation of pheochromocytomas and paragangliomas may differ based on patient presentation (eg, secretory vs nonsecretory). For patients with nonsecretory paragangliomas, these lesions are often incidentally discovered on CT scans or MR imaging of the abdomen and pelvis performed for alternate reasons. On CT scanning, paragangliomas and pheochromocytomas demonstrate avid contrast enhancement with delayed washout. On MR imaging, paragangliomas and pheochromocytomas demonstrate T1 hypointensity when compared with the liver and adrenal gland and have a characteristic high signal on T2-weighted images. Additionally, MR imaging may also demonstrate the so-called salt and pepper appearance of paragangliomas and pheochromocytomas owing to flow voids within the lesion from high vascularity, superimposed on the avid contrast enhancement[72] (**Fig. 9**). Although CT scans and MR imaging offer superb sensitivity and spatial resolution compared with molecular imaging modalities, they frequently are unable to definitively characterize a mass as a paraganglioma and/or a pheochromocytoma.[73] In such cases, a noninvasive molecular imaging evaluation is often preferred to an invasive percutaneous biopsy of these lesions secondary to concerns of precipitating a hypertensive crisis secondary to catecholamine

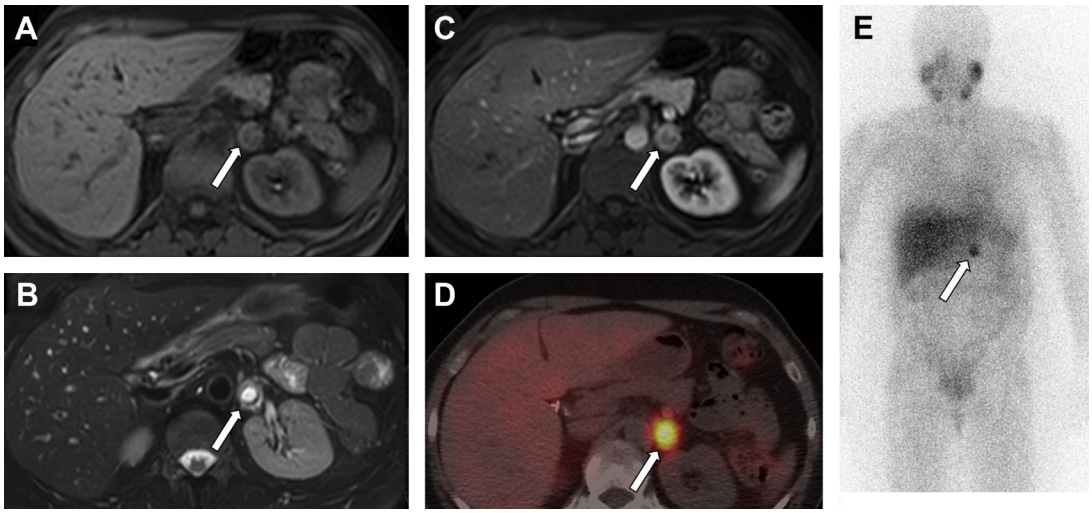


**Fig. 9.** Axial MR imaging with T1-weighted precontrast (*A*), arterial phase postcontrast (*B*), and T2-weighted (*C*) images demonstrate a T2 hyperintense enhancing left adrenal mass (*arrows*), which demonstrated marked activity of both SPECT/CT (*D*) and planar (*E*) images from subsequent [$^{123}$I]MIBG scan, confirming the diagnosis of pheochromocytoma.

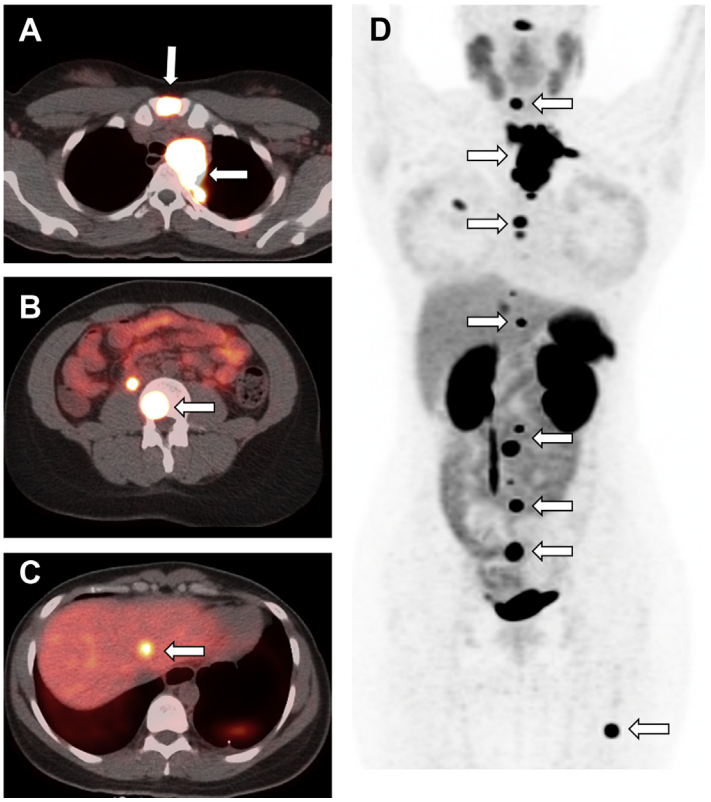


**Fig. 10.** Axial fused [$^{68}$Ga]DOTATATE-PET/CT (*A–C*) and maximum intensity projection image (*D*) in a patient with metastatic paraganglioma. Metastases (*arrows*) are present in the sternum, upper mediastinal and cervical lymph nodes, spine, liver, right, and left femur.

release during biopsy in a patient with pheochromocytoma who has not undergone periprocedural alpha-blockade.

Molecular imaging has long been the mainstay of noninvasive definitive diagnosis of paragangliomas and pheochromocytomas. For secretory pheochromocytomas, [$^{123}$I] or [$^{131}$I]meta-iodobenzylguanidine (MIBG) is a molecular imaging analog of norepinephrine that targets the presynaptic norepinephrine transporter.[74] This mechanism results in the accumulation of radiotracer in patients with hyperfunctioning lesions. After administration, patients are imaged with both planar gamma cameras and SPECT/CT scans to localize the lesion and any possible metastases. Early clinical trials are evaluating the potential use of therapeutic [$^{131}$I]MIBG for the treatment of metastatic and/or recurrent pheochromocytoma or paraganglioma.[75] This theranostic approach could expand utilization of MIBG scans, particularly given that currently [$^{177}$Lu]DOTATATE is only approved for use in GEP-NETs. However, for tumors that are nonsecretory, MIBG scans may be limited in their ability to detect and characterize lesions. Alternately, [$^{68}$Ga]DOTATATE-PET/CT scans can be used for imaging owing to overexpression of SSTRs at the cell surface of both pheochromocytomas and paragangliomas (**Fig. 10**). Although few studies have directly compared MIBG scans with [$^{68}$Ga]DOTATATE-PET/CT, early studies suggest that [$^{68}$Ga]DOTATATE-PET/CT scanning performs similarly in the evaluation and identification of the primary lesion, but superior to [$^{131}$I]MIBG and [$^{18}$F]FDG-PET/CT scan in the mapping of metastatic lesions.[76–78] [$^{18}$F]FDG-PET/CT scanning may also play a role for malignant paragangliomas and the information may be synergistic with findings on [$^{68}$Ga]DOTATATE-PET/CT scans for comprehensive staging and evaluation of patients.

## SUMMARY

NETs are a wide spectrum of disease that affect a broad range of organ systems throughout the body. Although varied in location, NETs tend to share common imaging features such as avid contrast enhancement and overexpression of SSTRs. However, malignant NETs may express only some or none of these features, and knowledge of NET pathology before imaging modality selection is important. Thus, imaging of NETs requires both standard anatomic and functional molecular imaging modalities to comprehensively

stage patients and make informed treatment decisions. As the roles of PRRT and theranostics expand, other NETs beyond GEP-NETs may be treated in a theranostic approach with both [$^{177}$Lu]DOTATATE and [$^{131}$I]MIBG.

## DISCLOSURE

The authors have nothing to disclose.

## REFERENCES


1. Dasari A, Shen C, Halperin D, et al. Trends in the incidence, prevalence, and survival outcomes in patients with neuroendocrine tumors in the United States. JAMA Oncol 2017;3(10):1335–42.
2. Expert Panel on Neurologic I, Burns J, Policeni B, et al. ACR appropriateness criteria((R)) neuroendocrine imaging. J Am Coll Radiol 2019;16(5S): S161–73.
3. Sundin A, Vullierme MP, Kaltsas G, et al, Mallorca Consensus Conference Participants European Neuroendocrine Tumor Society. ENETS Consensus guidelines for the standards of care in neuroendocrine tumors: radiological examinations. Neuroendocrinology 2009;90(2):167–83.
4. Cappelli C, Boggi U, Mazzeo S, et al. Contrast enhancement pattern on multidetector CT predicts malignancy in pancreatic endocrine tumours. Eur Radiol 2015;25(3):751–9.
5. George E, Wortman JR, Fulwadhva UP, et al. Dual energy CT applications in pancreatic pathologies. Br J Radiol 2017;90(1080):20170411.
6. Kamaoui I, De-Luca V, Ficarelli S, et al. Value of CT enteroclysis in suspected small-bowel carcinoid tumors. AJR Am J Roentgenol 2010;194(3):629–33.
7. Van Weyenberg SJ, Meijerink MR, Jacobs MA, et al. MR enteroclysis in the diagnosis of small-bowel neoplasms. Radiology 2010;254(3):765–73.
8. Thoeni RF, Mueller-Lisse UG, Chan R, et al. Detection of small, functional islet cell tumors in the pancreas: selection of MR imaging sequences for optimal sensitivity. Radiology 2000;214(2):483–90.
9. Anaye A, Mathieu A, Closset J, et al. Successful preoperative localization of a small pancreatic insulinoma by diffusion-weighted MRI. JOP 2009;10(5): 528–31.
10. Kang BK, Kim JH, Byun JH, et al. Diffusion-weighted MRI: usefulness for differentiating intrapancreatic accessory spleen and small hypervascular neuroendocrine tumor of the pancreas. Acta Radiol 2014; 55(10):1157–65.
11. Jang KM, Kim SH, Lee SJ, et al. The value of gadoxetic acid-enhanced and diffusion-weighted MRI for prediction of grading of pancreatic neuroendocrine tumors. Acta Radiol 2014;55(2):140–8.
12. Caramella C, Dromain C, De Baere T, et al. Endocrine pancreatic tumours: which are the most useful MRI sequences? Eur Radiol 2010;20(11):2618–27.
13. Sahani DV, Bonaffini PA, Fernandez-Del Castillo C, et al. Gastroenteropancreatic neuroendocrine tumors: role of imaging in diagnosis and management. Radiology 2013;266(1):38–61.
14. Tamm EP, Kim EE, Ng CS. Imaging of neuroendocrine tumors. Hematol Oncol Clin North Am 2007; 21(3):409–32, vii.
15. Subramaniam RM, Bradshaw ML, Lewis K, et al. ACR Practice Parameter for the Performance of Gallium-68 DOTATATE PET/CT for Neuroendocrine Tumors. Clin Nucl Med 2018;43(12):899–908.
16. Poeppel TD, Binse I, Petersenn S, et al. 68Ga-DOTATOC versus 68Ga-DOTATATE PET/CT in functional imaging of neuroendocrine tumors. J Nucl Med 2011;52(12):1864–70.
17. Deppen SA, Liu E, Blume JD, et al. Safety and Efficacy of 68Ga-DOTATATE PET/CT for diagnosis, staging, and treatment management of neuroendocrine tumors. J Nucl Med 2016;57(5):708–14.
18. Balon HR, Brown TL, Goldsmith SJ, et al. The SNM practice guideline for somatostatin receptor scintigraphy 2.0. J Nucl Med Technol 2011;39(4):317–24.
19. Portela-Gomes GM, Stridsberg M, Grimelius L, et al. Differential expression of the five somatostatin receptor subtypes in human benign and malignant insulinomas - predominance of receptor subtype 4. Endocr Pathol 2007;18(2):79–85.
20. Herrera-Martinez AD, Gahete MD, Pedraza-Arevalo S, et al. Clinical and functional implication of the components of somatostatin system in gastroenteropancreatic neuroendocrine tumors. Endocrine 2018;59(2):426–37.
21. Leijon H, Remes S, Hagstrom J, et al. Variable somatostatin receptor subtype expression in 151 primary pheochromocytomas and paragangliomas. Hum Pathol 2019;86:66–75.
22. Papotti M, Bongiovanni M, Volante M, et al. Expression of somatostatin receptor types 1-5 in 81 cases of gastrointestinal and pancreatic endocrine tumors. A correlative immunohistochemical and reverse-transcriptase polymerase chain reaction analysis. Virchows Arch 2002;440(5):461–75.
23. Mato E, Matias-Guiu X, Chico A, et al. Somatostatin and somatostatin receptor subtype gene expression in medullary thyroid carcinoma. J Clin Endocrinol Metab 1998;83(7):2417–20.
24. Schillaci O, Massa R, Scopinaro F. 111In-pentetreotide scintigraphy in the detection of insulinomas: importance of SPECT imaging. J Nucl Med 2000; 41(3):459–62.
25. Adams S, Baum RP, Hertel A, et al. Comparison of metabolic and receptor imaging in recurrent medullary thyroid carcinoma with histopathological findings. Eur J Nucl Med 1998;25(9):1277–83.

26. Whiteman ML, Serafini AN, Telischi FF, et al. 111In octreotide scintigraphy in the evaluation of head and neck lesions. AJNR Am J Neuroradiol 1997; 18(6):1073–80.
27. Nockel P, Babic B, Millo C, et al. Localization of insulinoma using 68Ga-DOTATATE PET/CT Scan. J Clin Endocrinol Metab 2017;102(1):195–9.
28. Rindi G, Klimstra DS, Abedi-Ardekani B, et al. A common classification framework for neuroendocrine neoplasms: an International Agency for Research on Cancer (IARC) and World Health Organization (WHO) expert consensus proposal. Mod Pathol 2018;31(12):1770–86.
29. Inzani F, Petrone G, Rindi G. The new world health organization classification for pancreatic neuroendocrine neoplasia. Endocrinol Metab Clin North Am 2018;47(3):463–70.
30. Walczyk J, Sowa-Staszczak A. Diagnostic imaging of gastrointestinal neuroendocrine neoplasms with a focus on ultrasound. J Ultrason 2019;19(78): 228–35.
31. McKenna LR, Edil BH. Update on pancreatic neuroendocrine tumors. Gland Surg 2014;3(4):258–75.
32. Tan EH, Tan CH. Imaging of gastroenteropancreatic neuroendocrine tumors. World J Clin Oncol 2011; 2(1):28–43.
33. Hill JS, McPhee JT, McDade TP, et al. Pancreatic neuroendocrine tumors: the impact of surgical resection on survival. Cancer 2009;115(4):741–51.
34. Wu J, Sun C, Li E, et al. Non-functional pancreatic neuroendocrine tumours: emerging trends in incidence and mortality. BMC Cancer 2019;19(1):334.
35. Modlin IM, Oberg K, Chung DC, et al. Gastroenteropancreatic neuroendocrine tumours. Lancet Oncol 2008;9(1):61–72.
36. Chang S, Choi D, Lee SJ, et al. Neuroendocrine neoplasms of the gastrointestinal tract: classification, pathologic basis, and imaging features. Radiographics 2007;27(6):1667–79.
37. Baxi AJ, Chintapalli K, Katkar A, et al. Multimodality imaging findings in carcinoid tumors: a head-to-toe spectrum. Radiographics 2017;37(2):516–36.
38. Lewis RB, Lattin GE Jr, Paal E. Pancreatic endocrine tumors: radiologic-clinicopathologic correlation. Radiographics 2010;30(6):1445–64.
39. Denecke T, Baur AD, Ihm C, et al. Evaluation of radiological prognostic factors of hepatic metastases in patients with non-functional pancreatic neuroendocrine tumors. Eur J Radiol 2013;82(10): e550–5.
40. Kumbasar B, Kamel IR, Tekes A, et al. Imaging of neuroendocrine tumors: accuracy of helical CT versus SRS. Abdom Imaging 2004;29(6):696–702.
41. Wong KK, Cahill JM, Frey KA, et al. Incremental value of 111-in pentetreotide SPECT/CT fusion imaging of neuroendocrine tumors. Acad Radiol 2010; 17(3):291–7.
42. Shaverdian N, Pinchot SN, Zarebczan B, et al. Utility of (1)(1)(1)indium-pentetreotide scintigraphy in patients with neuroendocrine tumors. Ann Surg Oncol 2013;20(2):640–5.
43. Sadowski SM, Neychev V, Millo C, et al. Prospective Study of 68Ga-DOTATATE positron emission tomography/computed tomography for detecting gastro-entero-pancreatic neuroendocrine tumors and unknown primary sites. J Clin Oncol 2016;34(6): 588–96.
44. Van Binnebeek S, Vanbilloen B, Baete K, et al. Comparison of diagnostic accuracy of (111)In-pentetreotide SPECT and (68)Ga-DOTATOC PET/CT: a lesion-by-lesion analysis in patients with metastatic neuroendocrine tumours. Eur Radiol 2016;26(3): 900–9.
45. Hilal T. Current understanding and approach to well differentiated lung neuroendocrine tumors: an update on classification and management. Ther Adv Med Oncol 2017;9(3):189–99.
46. Rosado de Christenson ML, Abbott GF, Kirejczyk WM, et al. Thoracic carcinoids: radiologic-pathologic correlation. Radiographics 1999;19(3):707–36.
47. Chong S, Lee KS, Chung MJ, et al. Neuroendocrine tumors of the lung: clinical, pathologic, and imaging findings. Radiographics 2006;26(1):41–57 [discussion: 57–8].
48. Chaer R, Massad MG, Evans A, et al. Primary neuroendocrine tumors of the thymus. Ann Thorac Surg 2002;74(5):1733–40.
49. Gaur P, Leary C, Yao JC. Thymic neuroendocrine tumors: a SEER database analysis of 160 patients. Ann Surg 2010;251(6):1117–21.
50. Moran CA, Suster S. Neuroendocrine carcinomas (carcinoid tumor) of the thymus. A clinicopathologic analysis of 80 cases. Am J Clin Pathol 2000;114(1): 100–10.
51. Nishino M, Ashiku SK, Kocher ON, et al. The thymus: a comprehensive review. Radiographics 2006;26(2): 335–48.
52. Walts AE, Frye J, Engman DM, et al. Carcinoid tumors of the thymus and Cushing's syndrome: clinicopathologic features and current best evidence regarding the cell of origin of these unusual neoplasms. Ann Diagn Pathol 2019;38:71–9.
53. Jeung MY, Gasser B, Gangi A, et al. Bronchial carcinoid tumors of the thorax: spectrum of radiologic findings. Radiographics 2002;22(2):351–65.
54. Gould PM, Bonner JA, Sawyer TE, et al. Bronchial carcinoid tumors: importance of prognostic factors that influence patterns of recurrence and overall survival. Radiology 1998;208(1):181–5.
55. Scarsbrook AF, Ganeshan A, Statham J, et al. Anatomic and functional imaging of metastatic carcinoid tumors. Radiographics 2007;27(2): 455–77.

56. Brown LR, Aughenbaugh GL. Masses of the anterior mediastinum: CT and MR imaging. AJR Am J Roentgenol 1991;157(6):1171–80.
57. Araki T, Sholl LM, Hatabu H, et al. Radiological features and metastatic patterns of thymic neuroendocrine tumours. Clin Radiol 2018;73(5):479–84.
58. Chiaravalloti A, Spanu A, Danieli R, et al. 111In-pentetreotide SPECT/CT in pulmonary carcinoid. Anticancer Res 2015;35(7):4265–70.
59. Guidoccio F, Grosso M, Maccauro M, et al. Current role of 111In-DTPA-octreotide scintigraphy in diagnosis of thymic masses. Tumori 2011;97(2):191–5.
60. Jindal T, Kumar A, Venkitaraman B, et al. Evaluation of the role of [18F]FDG-PET/CT and [68Ga] DOTATOC-PET/CT in differentiating typical and atypical pulmonary carcinoids. Cancer Imaging 2011;11:70–5.
61. Moore W, Freiberg E, Bishawi M, et al. FDG-PET imaging in patients with pulmonary carcinoid tumor. Clin Nucl Med 2013;38(7):501–5.
62. Erasmus JJ, McAdams HP, Patz EF Jr, et al. Evaluation of primary pulmonary carcinoid tumors using FDG PET. AJR Am J Roentgenol 1998;170(5): 1369–73.
63. Chan DL, Bernard E, Schembri G, et al. High metabolic tumour volume on FDG PET predicts poor survival from neuroendocrine neoplasms. Neuroendocrinology 2019. https://doi.org/10.1159/000504673.
64. Lococo F, Perotti G, Cardillo G, et al. Multicenter comparison of 18F-FDG and 68Ga-DOTA-peptide PET/CT for pulmonary carcinoid. Clin Nucl Med 2015;40(3):e183–9.
65. Chen H, Sippel RS, O'Dorisio MS, et al. The North American Neuroendocrine Tumor Society consensus guideline for the diagnosis and management of neuroendocrine tumors: pheochromocytoma, paraganglioma, and medullary thyroid cancer. Pancreas 2010;39(6):775–83.
66. Beard CM, Sheps SG, Kurland LT, et al. Occurrence of pheochromocytoma in Rochester, Minnesota, 1950 through 1979. Mayo Clin Proc 1983;58(12): 802–4.
67. Sutton MG, Sheps SG, Lie JT. Prevalence of clinically unsuspected pheochromocytoma. Review of a 50-year autopsy series. Mayo Clin Proc 1981; 56(6):354–60.
68. Erickson D, Kudva YC, Ebersold MJ, et al. Benign paragangliomas: clinical presentation and treatment outcomes in 236 patients. J Clin Endocrinol Metab 2001;86(11):5210–6.
69. Parenti G, Zampetti B, Rapizzi E, et al. Updated and new perspectives on diagnosis, prognosis, and therapy of malignant pheochromocytoma/paraganglioma. J Oncol 2012;2012:872713.
70. Lee JH, Barich F, Karnell LH, et al. National Cancer Data Base report on malignant paragangliomas of the head and neck. Cancer 2002;94(3):730–7.
71. Chrisoulidou A, Kaltsas G, Ilias I, et al. The diagnosis and management of malignant phaeochromocytoma and paraganglioma. Endocr Relat Cancer 2007;14(3):569–85.
72. Blake MA, Kalra MK, Maher MM, et al. Pheochromocytoma: an imaging chameleon. Radiographics 2004;24(Suppl 1):S87–99.
73. Baez JC, Jagannathan JP, Krajewski K, et al. Pheochromocytoma and paraganglioma: imaging characteristics. Cancer Imaging 2012;12:153–62.
74. Vallabhajosula S, Nikolopoulou A. Radioiodinated metaiodobenzylguanidine (MIBG): radiochemistry, biology, and pharmacology. Semin Nucl Med 2011; 41(5):324–33.
75. Noto RB, Pryma DA, Jensen J, et al. Phase 1 study of high-specific-activity I-131 MIBG for Metastatic and/or recurrent pheochromocytoma or paraganglioma. J Clin Endocrinol Metab 2018;103(1): 213–20.
76. Tan TH, Hussein Z, Saad FF, et al. Diagnostic performance of (68)Ga-DOTATATE PET/CT, (18)F-FDG PET/CT and (131)I-MIBG scintigraphy in mapping metastatic pheochromocytoma and paraganglioma. Nucl Med Mol Imaging 2015;49(2):143–51.
77. Jing H, Li F, Wang L, et al. Comparison of the 68Ga-DOTATATA PET/CT, FDG PET/CT, and MIBG SPECT/CT in the evaluation of suspected primary pheochromocytomas and paragangliomas. Clin Nucl Med 2017;42(7):525–9.
78. Han S, Suh CH, Woo S, et al. Performance of (68) Ga-DOTA-Conjugated somatostatin receptor-targeting peptide PET in detection of pheochromocytoma and paraganglioma: a systematic review and metaanalysis. J Nucl Med 2019;60(3):369–76.